UNIVERSITY OF BELGRADE
FACULTY OF PHYSICS

INNER-SHELL ACTION SPECTROSCOPY OF TRAPPED SUPSTANCE P PEPTIDE IONS AND THEIR NANOSOLVATED COMPLEXES

Iva Bačić, 7047/2014

Master Thesis
Belgrade, 2015

Abstract

We have performed near edge X-ray absorption fine structure action spectroscopy of both bare and nanosolvated gas-phase Substance P peptide ions, by coupling a linear quadrupole ion trap, equipped with an ESI source, to a soft X-ray beamline. By recording tandem mass spectra around the O K-edge of a nanosolvated protonated peptide, we attempted to determine the effects of nanosolvation on the action spectra and the fragmentation pattern. We observed two distinct resonant processes leading to increased water loss from the nanosolvated Substance P, which are related to K-shell excitation of oxygen atoms belonging either to the peptide bond or to the water cluster. Furthermore, we studied peptide fragmentation as a function of the activation photon energy, near the C, N and O K-edges. The fragmentation pattern strongly depends on the activation energy.

Acknowledgements

Firstly, I would like to express my sincere gratitude to my advisor dr. Aleksandar R. Milosavljević, who provided me an opportunity to participate in this work, and guided me through the whole course of this research with excellent help and great patience in correcting my writing. I would also like to thank my co-supervisor dr. Bratislav Marinković, for his assistance in the writing of this paper, along with dr. Aleksandar R. Milosavljević. My sincere thanks also go to mr. Miloš Ranković for great help in performing the experiment and processing the data, and dr. Alex Giulliani and dr. Cristophe Nicolas, with whom I worked during the experiment at the research facility SOLEIL for admitting me to their team and advising me during the beamtime. I am also grateful to dr. Viktor Cerovski for his help during the measurements and to the general SOLEIL staff for running the overall facility. Besides those who directly participated in the making of this work, I would like to thank the rest of my thesis committee: dr. Jelena Maljković, prof. dr. Goran Poparić, and prof. dr. Dragoljub Belić for their critical reading of the thesis and useful suggestion. Finally, I also thank dr. Sanja Tošić for useful advises and help with preparing the thesis.

This work was performed under the project 20140023 “Inner-shell spectroscopy of nanosolvated protein ions isolated in gas phase” at the SOLEIL synchrotron radiation facility and also supported by the Ministry of Education, Science and Technological Development, Serbia, under the project numbers 171020. The experimental setup has been developed with the support from the Agence Nationale de la Recherche Scientifique, France, under the project number ANR-08-BLAN-0065.

Publications

Gas-phase X-ray action spectroscopy of protonated nanosolvated substance P peptide around O K-edge,

I. Bačić, M. Lj. Ranković, F. Canon, V. Cerovski, C. Nicolas, A. Giuliani and A. R. Milosavljević,

Proc. WG2 Expert Meeting on Biomolecules, COST Action CM1204, XLIC - XUV/X-ray Light and fast Ions for ultrafast Chemistry, April 27-30, 2015, Book of Abstracts, Eds. Paola Bolognesi and Aleksandar Milosavljević, Poster presentation P08, p.71. http://www.xlic-wg2-2015.ipb.ac.rs/

Table of contents

1. Introduction

1.1. Gas-Phase X-ray Spectroscopy of Large Biomolecules

Amino acids are the structural units of a wide range of biomolecules. Due to their biological importance, amino acids and their polymers have great scientific appeal. Having in mind that the complex three-dimensional molecular structure of an amino acid polymer and its corresponding biological function is determined by the unique sequence of amino acids in the polypeptide chain, enduring research has been devoted to understanding the structural and dynamical properties of these molecules in order to accurately predict their biological function (see Ref[1] and references therein). Moreover, it has been shown that there is a strong correlation between the physicochemical properties and the three-dimensional structure of a biopolymer.[2] On the other hand, it has been also shown that the presence of water molecules plays an important role in determining behavior of biomolecules.[3] Therefore, studying these effects opens up the possibility of gaining better insight into the physicochemical properties of biomolecules and their biological functions.

A widely used method for determining the chemical and electronic structure of a given sample is X-ray absorption spectroscopy[4]. However, several difficulties arise when treating large biomolecules (also called biomacromolecules) with X-rays. First of all, although these molecules are not isolated in nature, studying them in condensed or liquid states brings several drawbacks. The problem with treating condensed matter samples (such as thin organic films) with X-rays lies in the fact that biologically relevant molecules are easily damaged when exposed to such energetic radiation (see Ref.[1] and references therein). If molecules need to be treated with long and intensive soft X-ray beams for obtaining accurate results, this approach to studying biomacromolecules is usually futile, as it results in chemical transformations of the original sample. Furthermore, spectra obtained by studying condensed matter or liquid samples of biomolecules may be unreliable due to other compounds and impurities present in the sample, which consequently may alter the results. Applying spectroscopic methods to biomolecules isolated in the gas phase would bypass these difficulties; however, large biomolecules cannot be easily transferred to the gas phase remaining intact. This has been one of the largest obstacles in performing gas-phase X-ray spectroscopy of biomacromolecules.[1]

Contemporary methods for studying the activity of biomolecules and their structure

are based on synchrotron inner-shell spectroscopic techniques, such as near-edge X-ray absorption fine structure (NEXAFS) spectroscopy.[5] The onset of third generation synchrotron sources made NEXAFS spectroscopy a widely popular technique for studying chemical and electronic properties of biomolecules, as third generation synchrotron radiation sources provide intense, high resolution and tunable X-ray beams. A novel approach to performing inner-shell spectroscopy of large biomolecules isolated in the gas phase has been recently developed and successfully performed on cytochrome *c*, a protein of molecular mass cca 12 kDa.[1] Based on coupling a highly selective linear quadrupole ion-trap spectrometer, equipped with an electrospray ionization source, with a soft X-ray beamline, this method allows studying isolated targets practically regardless of size and charge states while being performed under well-defined conditions.

Having in mind that the natural environment of biomacromolecules are aqueous solutions, it is important to understand the effect of the solvent on the structure and physicochemical properties of the biomolecule and its function.[3,6] Therefore, it is necessary to somehow bridge the gap between properties in solution and the gas phase.[4] Recently developed experimental techniques created novel possibilities for obtaining a better insight into the effect of a small and well-defined number of water molecules on biomolecular properties and interactions, such as the dynamics of chemical reactions[7,8], the structure of peptides[9] and stability of fragile non-covalent complexes[3]. Introducing a small number of solvent molecules is called nanosolvation or microsolvation. For example, a peptide dimer isolated in the gas phase can be significantly stabilized by nanosolvation[3]. Therefore, studying the influence of a small, controllable number of solvent molecules on physicochemical properties of biomolecules may finally lead to binding the gap between research conducted in the gas phase and in solutions.

1.2. The physical background of the method

Although first intended for analyzing molecules composed of atoms with low atomic numbers, present-day as NEXAFS spectroscopy is a powerful tool suitable for studying much more intricate systems. In our present approach, the action NEXAFS spectroscopy is used for analyzing biomacromolecules in the gas phase by probing the core levels of atoms in the molecule and measuring the relative yield of different formed ionic compounds as a

function of the photon energy. An overview of the method will be given at the end of this section.

Spectra obtained by exposing a sample to X-rays reveal that there are sudden increases of X-ray absorption at certain energies. This sudden increase corresponds to the energies at which inner-shell electrons absorb X-ray photons. Having in mind that each element has specific energies at which this absorption happens, this method is element specific and can be used for identifying the elemental structure of a sample. Absorption edges are named according to the principle quantum numbers of excited electrons, so the absorption edge of 1s electrons is named the K-edge, the absorption edge of 2s and 2p electrons is named the L-edge and so forth. It is important to note that the term "absorption edge" refers to a range of energy values in the vicinity of the energy at which photons are absorbed by core electrons upon X-ray irradiation (as opposed to that specific energy value at which absorption happens). By convention, the width of this range is 50eV and the structure within range is referred to as near-edge X-ray absorption fine structure, hence the name NEXAFS. The fine structure is a consequence of electron excitations from core shells into unoccupied molecular orbitals.[10,11]

A typical measurement involves irradiating the sample with monochromatic X-rays in order to probe transitions from the K-edge core shell of an atom.[4 2] In the soft X-ray energy range (up to 2000eV), the dominant process is photoabsorption which produces a vacancy in the K-shell, relaxed either by a (normal) Auger process or by capturing an electron from a higher-energy shell followed by the emission of a fluorescent photon. This means that X-ray beams are capable of exciting a 1s core electron either to a bound higher energy shell or to the continuum, depending on whether the energy is below or above the ionization threshold, respectively. The excited 1s electron "leaves the atom" when the absorbed photon energy is larger than the one needed to ionize the molecule, while it stays within the molecular system occupying a discrete available energy level if the energy is not sufficient for ionization. A graphic representation of these two processes is provided in figure 1.1.

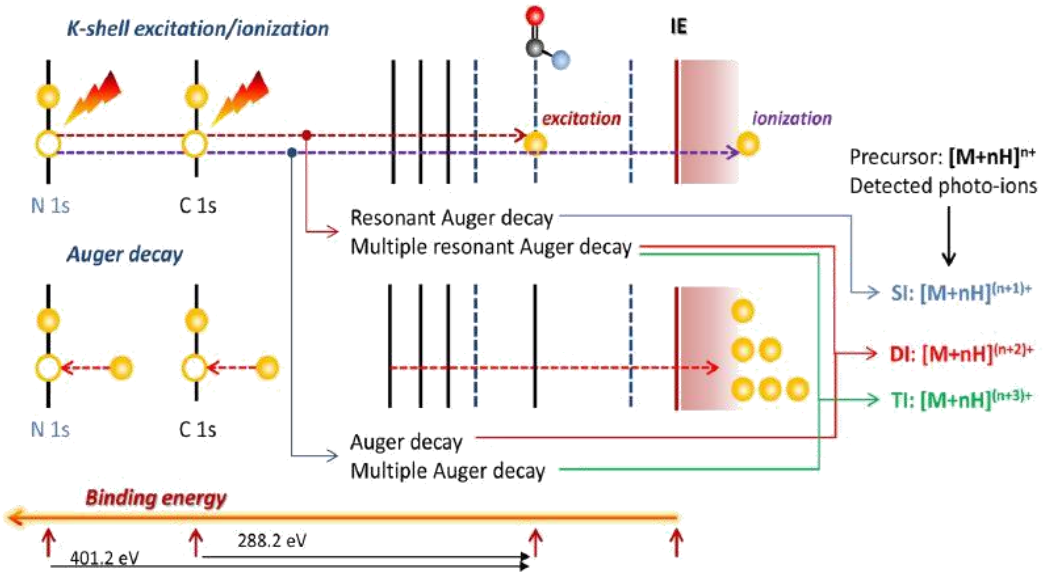

Figure 1.1: Schematic representation of the X-ray K-shell excitation/ionization of a protein, adopted from[2]

Below the ionization threshold, the core electron resonantly absorbs the photon and is excited to an unoccupied bonding molecular orbital. This state is very unstable and dominantly decays by the core vacancy being filled by an electron from the outer shell, while the system relaxes by ejecting an electron (the Auger electron), so this is a resonant Auger process. Note that it is also energetically possible to eject more than one Auger electron - a multiple resonant Auger process. When the incident photon energy is above the K-shell ionization threshold, the 1s electron is directly ejected into vacuum (a photoelectron) and the system is relaxed by a normal Auger decay. It is important to note that single ionization of the target can be produced only through the resonant Auger decay (1s electron excitation to an unoccupied molecular orbital). Therefore, the single photoionization yield reproduces a NEXAFS spectrum

A prominent method for extracting ions directly from a solution into the gas phase is electrospray ionization (ESI)[12,13]. ESI enables keeping large molecules intact, which makes it an appealing tool for studying the structure of biopolymers. Additionally, ion trapping devices provide another prosperous contribution to the possibility of performing inner-shell X-ray spectroscopy of large targets, as they allow performing mass and charge selected spectroscopy. Thus, equipping an ion trap with an ESI source creates a powerful device which can be coupled to a soft X-ray synchrotron beamline in order to perform

inner-shell X-ray spectroscopy.[1]

In the present experiment, electrosprayed ions are selected and stored in a linear ion trap. Upon reaching the optimal capacity of the ion trap, the contents of the trap is irradiated by soft X-rays for a controlled amount of time, after which the products can be analyzed using the mass spectroscopy. In tandem mass spectroscopy (MS^2), a desired ionic compound is isolated (by using an ion trap for example), activated (by using X-rays in our case) and mass analyzed. The basic idea of NEXAFS MS^2 spectroscopy is to record tandem mass spectra obtained after X-ray activation of the precursor ions as a function of the photon energy scanned around the C, N and O K-edges. The procedure can be repeated several times for the same photon energies in order to obtain satisfactory accurate results. Monitoring each process as a function of the X-ray photon energy is achieved by performing this procedure for different energies within the desired energy range. Third generation synchrotron facilities produce very bright and energy-resolved X-rays, so the measurement can be executed with small energy steps. The product ions detected after the interaction of X-rays and the contents of the trap can be used to derive partial ion yields over the photon energy range of interest, making this method an action spectroscopic method. A schematic representation of NEXAFS MS^2 is shown in figure 1.2.

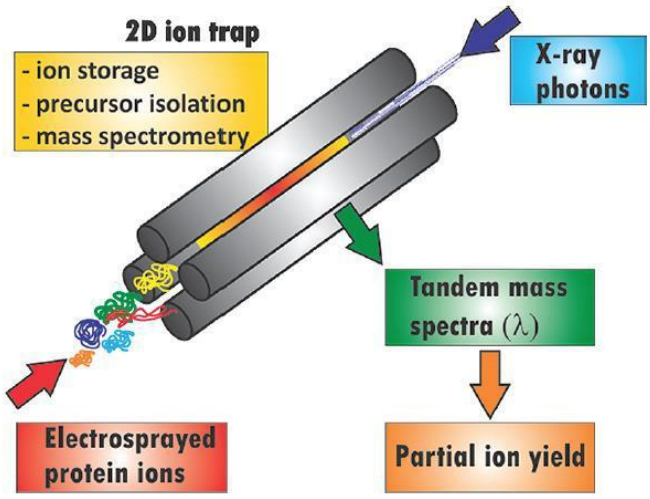

Figure 1.2: A schematic representation of the coupling of a linear quadrupole ion trap with an X-ray beamline used to obtain MS^2 spectra and partial ion yield spectra, adopted from [1]

Single ionization (SI) processes are necessarily triggered by resonant excitations of the core electron, making the normalized partial ion yield spectra for detected SI ions the NEXAFS action spectra. The double ionization (DI) of the precursor can be a result of either normal Auger ionization or resonant multiple resonant Auger ionization. The most probable resonant Auger excitation process is the ejection of only one Auger electron; however, multiple ionization processes can also happen with a smaller probability. As the abundance of DI ions suddenly increases when the ionization threshold is reached, the intensity of DI ions as a function of photon energy can be used for measuring the ionization threshold.

MS^2 NEXAFS action spectroscopy of trapped ions is a promising method for studying biologically relevant molecules. The growing interest in gas-phase spectroscopy of biomolecules is based on the idea that these results might provide fundamental insight into the structure and physicochemical properties of compounds. In addition to this, these results also provide reliable data sets on the interaction of studied compounds with X-ray irradiation, which may perhaps turn out to be a good reference point for theoretical modeling of biological matter.[5]

1.3. Substance P peptide

A vast number of biologically relevant molecules are composed of amino acids. When there is a chemical reaction between the carboxyl group (-COOH) of one amino acid and the amino group ($-NH_2$) of another, they form chemical covalent bonds named peptide bonds.[14] The remainder of amino acid molecules after removing the elements of water in order to bond with other amino acids is called an amino acid residue.[15] Molecules composed of short chains of amino acid residues linked by peptide bonds are called peptides.[16,17] All noncyclic peptide molecules have an N-terminal and C-terminal residue at the ends of the peptide – they are terminated by a free carboxyl group and a free amine group[15]. By convention[14], the beginning of a peptide is its N-terminal and the end is its C-terminal. Every peptide must contain hydrogen, carbon, nitrogen and oxygen and may contain other elements besides these. The backbone of a polypeptide is defined as the repeated sequence of the amide N atom, the central C atom and the carbonyl C atom of each amino acid residue in the chain.[14] The sidechains of the molecule are the atoms

attached to the central C atoms of the backbone.[14] Peptides can have an amide group added to the end of a polypeptide chain – this is called an amidation.[18]

Substance P is a peptide composed of a chain of 11 amino acid residues, namely: Arginine, Proline, Lysine, Proline, Glutamine, Glutamine, Phenylalanine, Phenylalanine, Glycine, Leucine and Methionine, with an amidation at the C-terminus: Arg-Pro-Lys-Pro-Gln-Gln-Phe-Phe-Gly-Leu-Met-NH_2.[19] The three-dimensional structural formula of Substance P is given in figure 1.3.

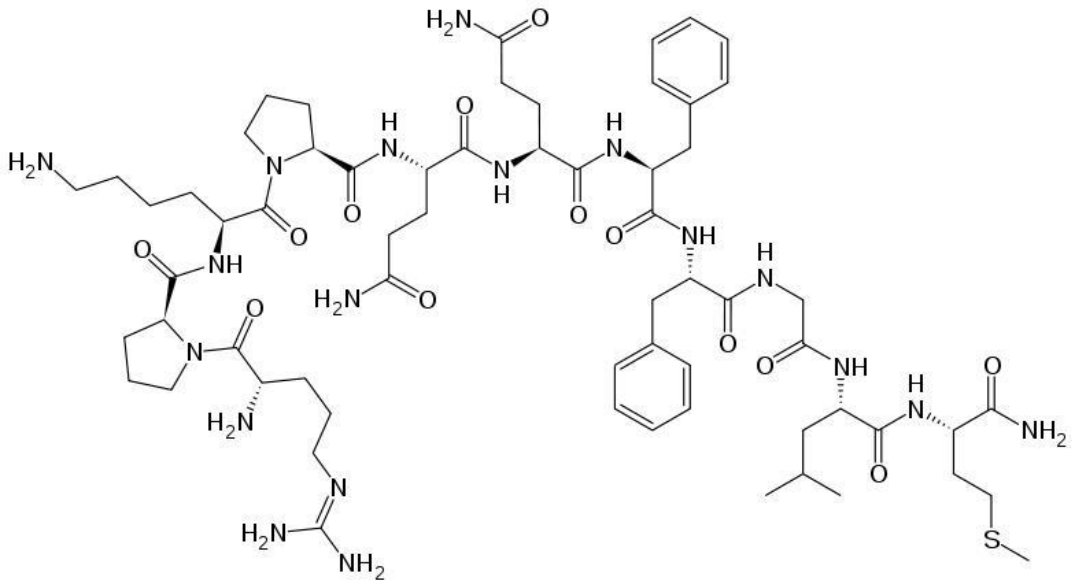

Figure 1.3: The three-dimensional structural formula of Substance P *(Wikimedia Commons / Public Domain)*

The chemical formula and molar mass of Substance P are $C_{63}H_{98}N_{18}O_{13}S$ and 1347.63 g/mol, respectively[20]. It has been shown that the conformation of Substance P appears to be strongly dependent upon the solvent used and the lipid environment in which this peptide is in.[21]

Substance P is a neuropeptide according to its biological function.[21,19] It is found in the brain and spinal cord and acts both in the peripheral nervous system and the central nervous system of the human body.[19] The clinical significance of performing research on Substance P lies in its association to human pathophysiology: it is shown to be associated with pain[22], inflammatory diseases[23,24], the regulation of stress-related anxiety and depression[25], major depressive disorder[26,27], PTSD[26] and many other medical conditions[21].

Substance P has become a model system for different spectroscopic techniques.[28] In recent years, the fragmentation of Substance P upon photoabsorption has been the subject of many studies. Distinct fragmentation regimes are observed, depending on whether the energy is below or above the ionization threshold.

2. Experimental setup

2. 1. Idea of the experiment

The approach used in this experiment provides the means to perform inner-shell spectroscopy of large biomolecular ions in the gas phase. Briefly, the NEXAFS action spectroscopy procedure is carried out by coupling a linear quadrupole ion trap equipped with ESI source to a soft X-ray synchrotron beamline. The ESI technique leaves large molecules intact while transferring them into the gas phase, making it a suitable method for generating gas-phase Substance P ions. The trapped mass/charge (m/z) selected electrosprayed precursor ions are activated by the X-ray beam. The products of interaction are analyzed by using mass spectrometry. Tandem mass spectra, recorded as a function of the photon energy around the C, N and O K-edges, are used to extract action NEXAFS spectra by measuring the relative abundance of the photoions according to their m/z values.

2.2. Electrospray ionization

ESI[12,13], in which gas-phase ions are created by exposing ions from a liquid solution to a high voltage, is a widely used method in the spectroscopy of biomacromolecules. The main advantage of ESI is the possibility of producing intact large molecular ions and in large charge states. ESI process consists of these three key steps[29,12]:

1. The production of charged droplets,
2. Size reduction of the charged droplets,
3. The production of desolvated gas-phase ions.

A simplified scheme of the whole process is given in figure 2.1. During the first step, a solution containing the substance is injected into a capillary under high voltage, leading to the ionization of analyte molecules. These ions are separated according to charge as a result of an electric field which forms within the solution. Affected by this field, the electrolyte ions move towards the electrode which is charged oppositely from the potential at which the capillary is set, which causes the accumulation of ions at surface of the liquid

in the tip of the capillary. The electrostatic force counteracts the surface tension and tends to deform the shape of the surface. As the voltage increases, the deformation becomes more prominent, finally leading to a cone-like shape with convex sides and a rounded tip – the Taylor cone. Upon reaching the threshold voltage at which the electrostatic force and the surface tension are in equilibrium, liquid jets are fired from the tip as a result of the liquid being attracted to the oppositely charged electrode by the electrostatic force – the solution is sprayed into droplets which are electrically charged at their surface, hence the name electrosprayed.

The second step begins with the collision of the ejected liquid jets with surrounding neutral gas molecules. During these collisions, the solvent evaporates, leaving smaller droplets with the same charge, increasing the charge surface density. When the balance between the surface tension of the droplets and the electrostatic force is disrupted – this is called the Rayleigh limit – the droplets fission into smaller droplets due to electrostatic repulsion. These droplets can go through further fragmentation until a desired droplet size is reached.The last step consists of removing the solvent from these charged droplets by further evaporation and fission, finally leading to the formation of ions isolated in the gas phase.

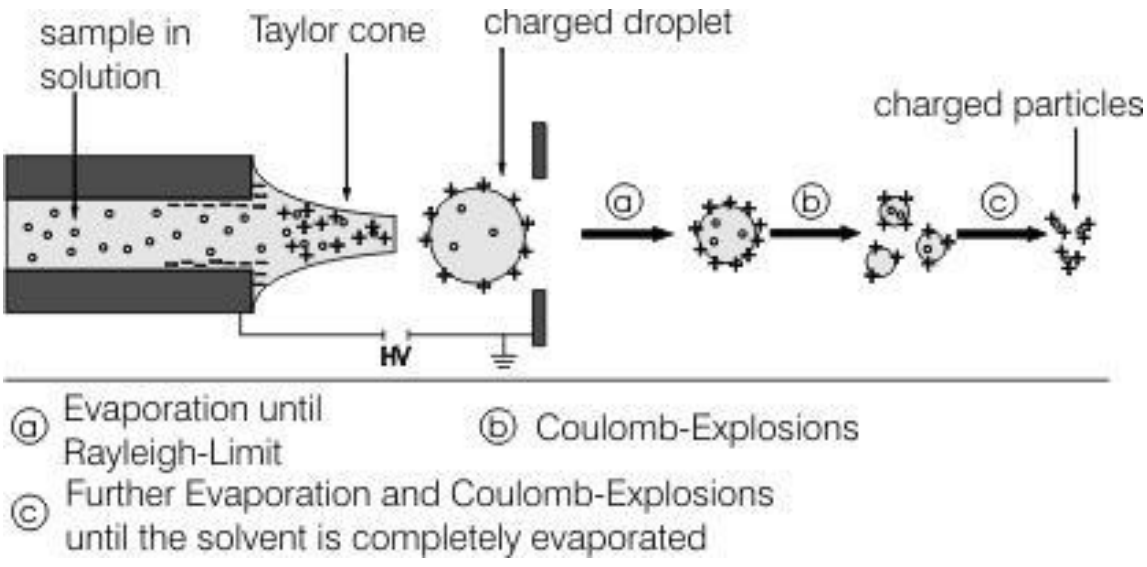

Figure 2.1: A simplified scheme of the process of electrospray ionization, adopted from [30]

2.3 Ion Guiding and Ion Trapping –Thermo LTQ Ion Mass Spectrometer

ESI sources can be conjoined with ion trap spectrometers to confine and preserve the ions in the trap, and analyze the contents of the trap. A popular contemporary ion trap is the linear quadrupole trap, which combines static direct current electric fields with radio frequency oscillating electric fields to trap ions by creating a potential well which confines them[31]. As the name suggests, these devices use a quadrupole electric field to trap ions (the total charge and dipole moment of a system that generates a quadrupole field is always zero, while the quadrupole moment is always nonzero). The mechanism of radial and axial ion trapping by the Thermo Scientific™ LTQ XL™ ion trap mass spectrometer[32], used in the present work, will be briefly explained in the following paragraph. This type of trap confines ions radially and axially:

- Radial confining is achieved by applying alternating (radio frequency) high voltage to two pairs of conducting rods (see figure 2.2). The voltage applied to one pair of opposite rods is different from the voltage applied to the other pair, making the ions simultaneously attracted and repulsed by opposite rods, which leads to their oscillations in a two-dimensional radio frequency electric field. This field is perpendicular to the ion path axis. Ideal quadrupole fields are generated by parabollicaly shaped electrodes.
- Axial confining is achieved by applying additional DC stopping potentials to the end electrodes.

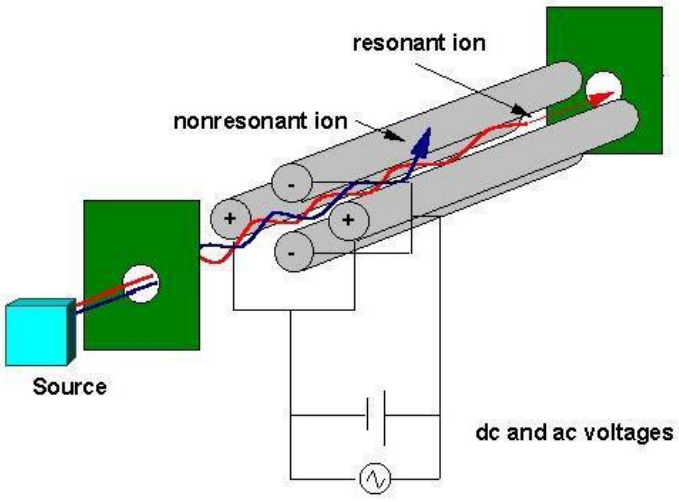

Figure 2.2: A simplified scheme of a linear quadrupole trap, adopted from[33]

Besides being storage devices, quadrupole ion traps also function as tandem mass spectrometers.[34] In quadrupole ion trap mass spectrometry, the ions are trapped in the same place while the steps of MS^2 are separated in time, which makes this method a tandem-in-time mass spectrometry. LTQ mass spectrometry consists of the following three time-separated steps:

1. The isolation of ions,
2. Excitation and fragmentation of initial ions,
3. Mass analysis of the produced ions.

Upon reaching the trap capacity, the contents are mass-analyzed by applying gradual changes to the electric field: the stability of ion paths in an electric field depends on their mass-to-charge ratios, so the ions leave the trap and hit the detector in order of their m/z ratios.

The instrument used in this setup is a commercial linear quadrupole trap mass spectrometer – the Thermo Finnigan LTQ XL[35] manufactured by Thermo Scientific™ (shown in figure 2.3).

Figure 2.3.: The Finnigan LTQ XL linear quadrupole ion mass spectrometer (adopted from[35])

In addition to the quadrupole electrodes, end electrodes are used to reduce edge effects. Each of the three sections (front, center and back) has DC voltages used for axial trapping by adjusting the potential of the center section to be lower than the potential of the front and back sections. Opposite quadrupole rods in each section are electrically connected. All pairs of rods are subjected to AC voltages of the same amplitudes, but the

sign of the voltage is opposite for opposite rods. These rods produce a two-dimensional quadrupole field in the ion trap, which confines ions in stable oscillatory trajectories. The ions are ejected from the trap from the center section, through two rods with slits, named exit rods. A scheme of the rod assembly used in this spectrometer is shown in figure 2.4.

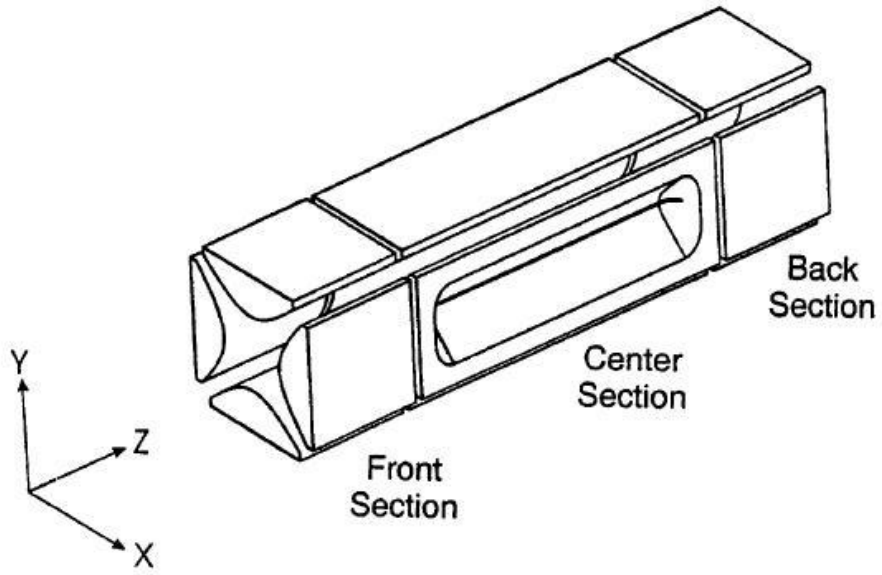

Figure 2.4: Schematic drawing of the LTQ XL ion trap used in the present experiment, adopted from[35]. The ions are ejected from the trap from the side from the center section.

The LTQ system consists of a syringe pump, an MS detector and an automatized data system (see figure 2.5). In our experimental procedure, the solution is directly infused into the spectrometer using a syringe pump, where it is ionized in the atmospheric pressure ionization (API) source, configured to work as an ESI source. The generated ions are guided through ion optics to the trap, where they can be selected and analyzed according to their mass-to-charge ratios, and ejected from the analyzer towards detectors. After ejection, they strike an ion detector. The ion detection system amplifies the signal produced by the ions and analyzes them using the LTQ Xcalibur® data system.

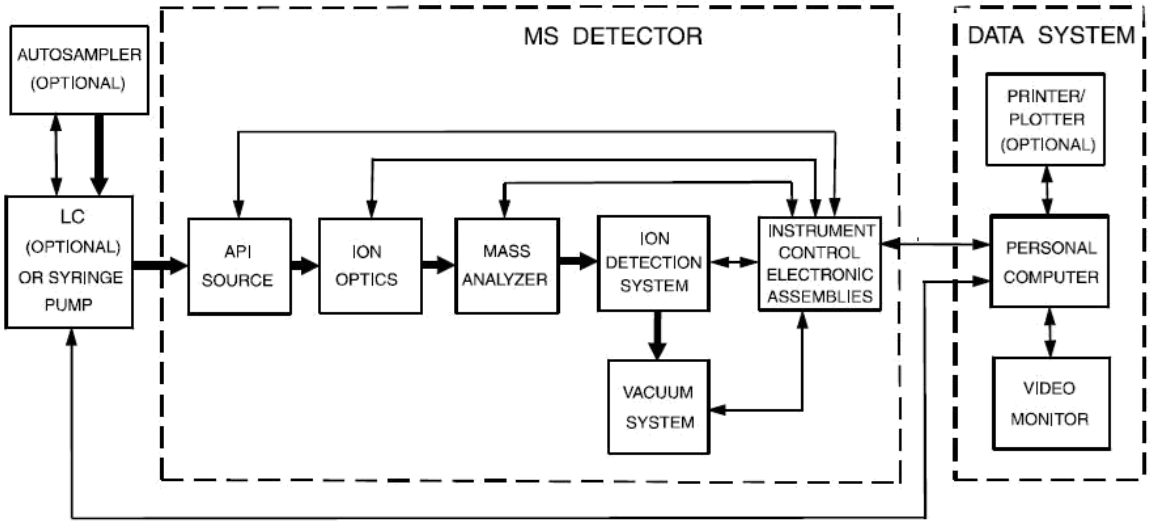

Figure 2.5: Functional block diagram of the LTQ system. The broad, single-headed arrows represent the flow of sample molecules through the instrument. The narrow, double-headed arrows represent electrical connections; adopted from [35].

2.4. SOLEIL synchrotron radiation facility

Synchrotron radiation (SR) is electromagnetic radiation which occurs when charged particles, radially accelerated to relativistic velocities, lose energy by emitting photons along their trajectories. SR is characterized by[5]: wide energy ranges, high brilliance, time structure of the pulsed light and adjustable polarization.

The measurements for this study were performed at the storage ring synchrotron radiation facility SOLEIL, located in Saint-Aubin in the Essonne département near Paris, France.[36] The name SOLEIL is a French acronym – „Soleil“ translates as "Sun" in French – for **S**ource **o**ptimisée de **l**umière d'**é**nergie **i**ntermédiaire du **L**URE[36] (LURE optimised intermediary energy light source), where LURE stands for **L**aboratoire pour l'**u**tilisation du **r**ayonnement **é**lectromagnétique (Laboratory for the use of electromagnetic radiation).

SOLEIL is a third generation synchrotron, characterized by very bright and energy-resolved beams. Its nominal energy is 2.75 GeV and it covers a wide spectral source range – from infrared (1 eV) to hard X-rays (50 keV). The circumference of the synchrotron is 345 m and its diameter is 113 m. The SOLEIL synchrotron facility provides a wide range of possibilities for both fundamental and applied research (such as research in physics, chemistry, life sciences, pharmacy, medicine, nanotechnologies, etc.).[36]

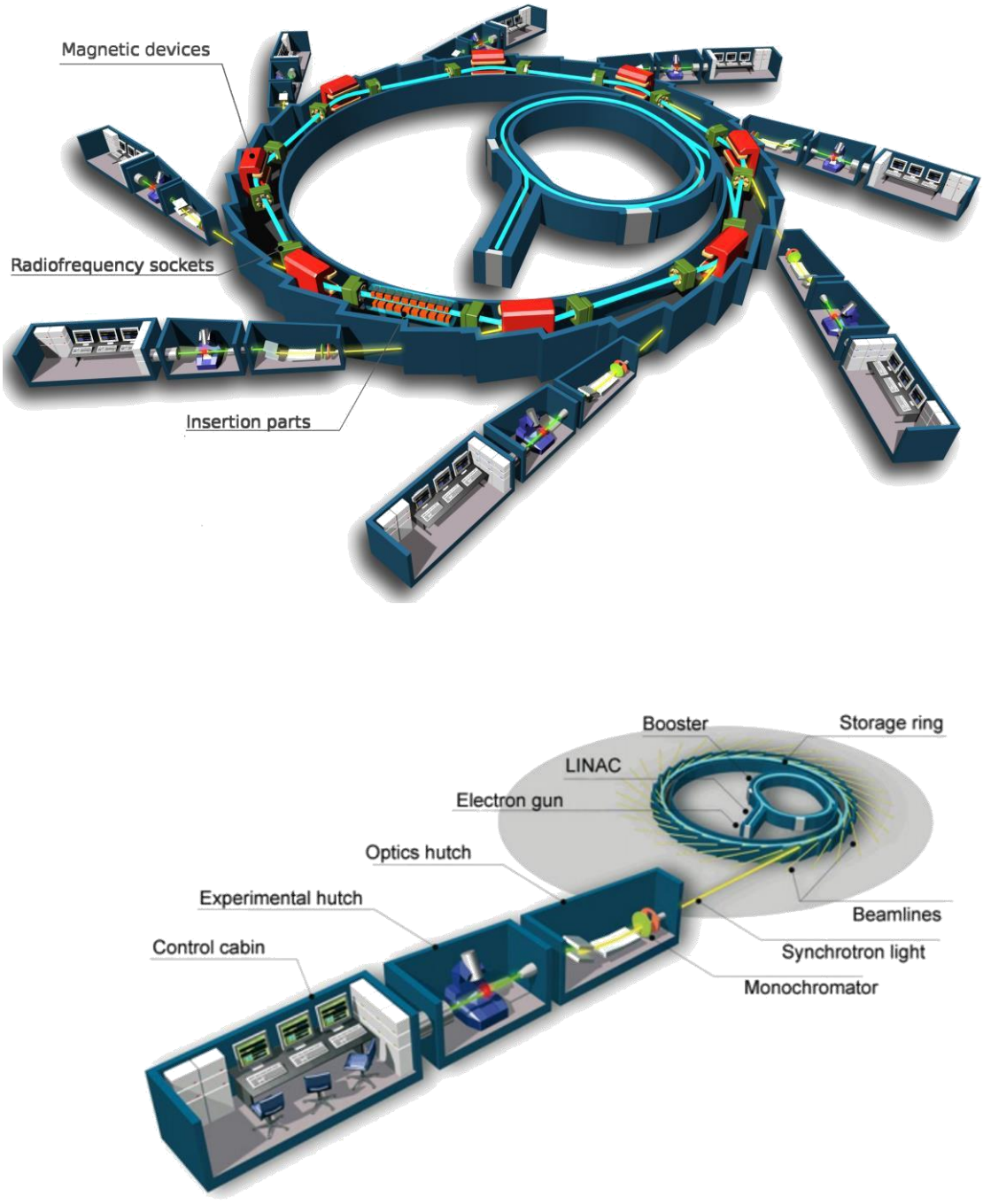

Figure 2.6.: A schematic representation of the SOLEIL synchrotron facility, adopted from[37,38]

The production of synchrotron radiation will briefly be explained in this paragraph (see figure 2.6 for schematic representations of the SOLEIL synchrotron facility and its beamlines).[36,39] The process begins with firing electrons from an electron gun and accelerating them up to the initial energy of 100 MeV in a 16 m long linear accelerator

(linac). After leaving the linac, the electron beam enters a second, circular accelerator, called the booster – a 157 m circumference synchrotron which boosts the energy level of the beam up to the SOLEIL operating value of 2.75 GeV. The beam characteristics are fine tuned in the booster. These high energy electrons then enter a 5 cm diameter tubular storage ring, in which they spend hours circulating at relativistic speeds. During this time, the relativistic electrons lose energy in the form of electromagnetic synchrotron radiation (SR), emitted tangentially to the direction of the beam. SR is produced in bending magnets and in two types of magnetic insertion devices: undulators and wigglers. The use of insertion devices is a significant improvement in SR, compared to second generation synchrotrons, where the radiation was generated only by bending magnets. Both types of insertion devices consist of periodic structures of dipole magnets which force the electrons to move along an oscillatory path (with different amplitudes). Undulators produce narrow energy bands of radiation and, increase the flux. The photon beams are finally directed towards the beamlines – the laboratories of SR facilities, each characterized by specific beam spot sizes, photon energy ranges and methods of analysis. A beamline is usually a set of the optics hutch cabin, the experimental hutch cabin and the control cabin, which are used for guiding and focusing the photon beam.

2.5. PLEIADES soft X-ray beamline

The present experiment has been performed on the PLEIADES soft X-ray beamline at the SOLEIL synchrotron radiation facility. PLEIADES is an acronym for „**P**olarized **L**ight source for **E**lectron and **I**on **A**nalysis from **D**iluted **E**xcited **S**pecies“. As the name suggests, this beamline is used for the spectroscopy of diluted samples. The technical details of this beamline are given in table 2.1., adopted from [40].

The photon beam is monochromatized using a plane grating monochromator. A scheme displaying the key elements of PLEIADES is given in figure 2.7.

Table 2.1: The technical characteristics of the PLEIADES beamline, adopted from [41].

Energy range	**10 eV - 1000 eV**
Resolving power	**15000 (10 eV - 40 eV), 20000 - 100000 (35 eV - 1000 eV)**
Source	**Electromagnetic HU256 (256 mm period) and Apple II permanent magnet HU80 (80 mm period) undulators**
Flux @ first optical element	**About $1.2 \cdot 10^{+15}$ Photons/s/0.1% BW @ 100 eV**
Optics	**PGM using varied line spacing (VLS) & varied groove depth (VGD) technologies with no entrance slit**
Sample Environment	**Differentially pumped gas cell for high resolution electron spectrometer** **Continuous measurement of the beam intensity (I_0)** **ECR ion source** **Gas inlet systems for the electron spectrometer and EPICEA coincidence setup** **Multi-purpose source chamber to generate beams of molecules, clusters and nanoparticles under vacuum**
Beam size at sample	**50(H)x30(V) μm^2 on branch N°2 ; 180(H)x100(V) μm^2 on branch N°3**
Beam divergence at sample (maximum)	**9mrad (H) - 4mrad (V) on branch N°2 ; 2mrad (H) - 0.6 mrad (V) on branch N°3**
Flux on sample	**About $1 \cdot 10^{+13}$ Photons/s/0.1% BW**
Detectors	**High resolution electron spectrometer, Electron - ion coincidence setup with PSDs**
Polarization	**10 - 40 eV (linear H, V); 35 - 1000 eV (linear H, V, tilted, elliptical)**

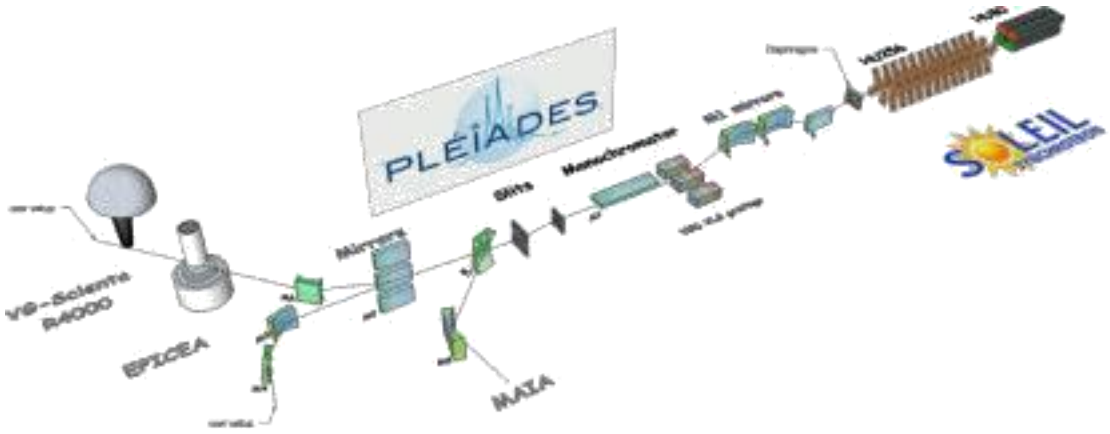

Figure 2.7.: A scheme of the PLEIADES beamline, adopted from [40].

2.6. Coupling the LTQ XL with the PLEIADES beamline – Experimental realization

The crucial element in the action NEXAFS spectroscopy method used in this work is the coupling of an ion trap spectrometer to a synchrotron beam. This pioneering experiment has been originally performed in VUV[42,43] and soon after in soft X-ray photon domain [1]. A simplified scheme of the experimental setup is given in figure 2.8.

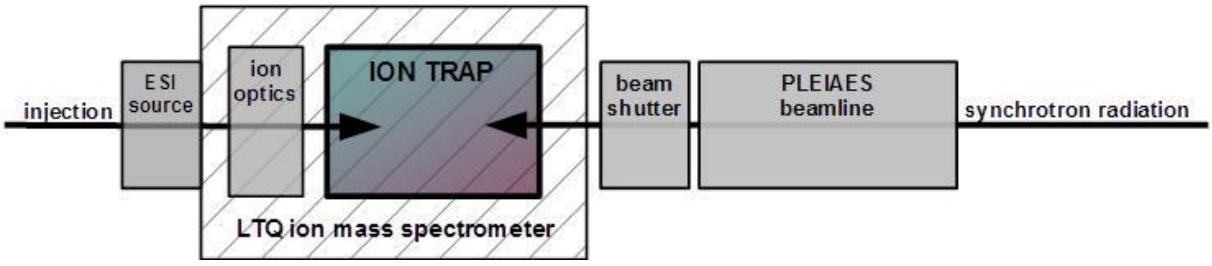

Figure 2.8: A simplified scheme of the experimental setup.

The LTQ XL was mounted on a supporting frame allowing a fine sub-millimeter tuning of its position in order to achieve a maximal overlap of the photon flux with the trapped ion packet, so to optimize the signal-to-noise ratio. The pressure difference between the beamline (10^{-9} mbar) and the LTQ XL (10^{-5} mbar of helium in the main LTQ chamber) was accommodated using a differential pumping stage. The desired precursor ions were generated by an ESI source which was connected to the LTQ XL. Substance P

was provided by Sigma Aldrich in powder form. Substance P ions were electrosprayed from a water solution of Substance P (concentration 100 mol/l), with the ion injection time set to 100 ms. These ions were injected through the front side of the trap while it was irradiated by a monochromatic X-ray beam from its back side in order to activate precursor ions confined in the ion trap. The LTQ XL has a helium bath for preserving high ionic densities with limited charge. The irradiation was controlled by a mechanical shutter, which was triggered by the LTQ XL and programmed to be open during a predefined time interval – the irradiation time– after which the contents of the trap were analyzed. The LTQ XL was adjusted to generate a pulse, allowing a delay before recording the spectra – the purpose of this delay is to minimize background noise in the measurement. Tandem mass spectra were recorded as a function of the photon energy in energy steps of 0.5 eV or 1 eV in the vicinity of the C, N and O K-edges. The procedure used to extract the action spectra from these results is explained in section 2.7. The LTQ mass spectrometer is placed downstream the WG Scienta setup (see figure 2.7). The whole process is synchronized and automatized by home-made software. A photo of the experimental setup is given in figure 2.9.

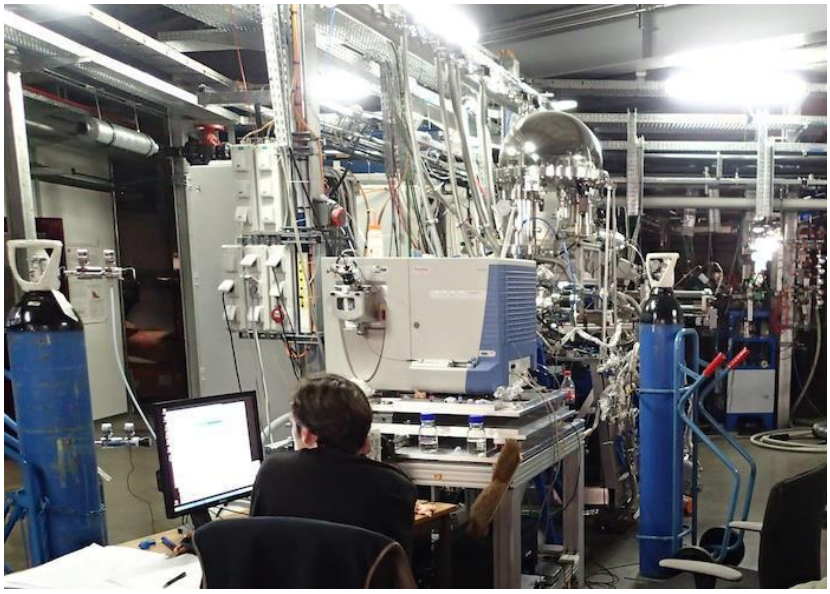

Figure 2.9: A photo of the experimental setup – coupling the LTQ XL mass spectrometer mounted on a dedicated supporting frame with the PLEIADES beamline at the SOLEIL synchrotron facility.

2.7. Experimental procedure and extraction of action spectra

The experimental procedure consists of the following sequence of events:

1. The beamline energy is set to a desired value.
2. The Substance P solution is administered using a syringe pump connected to the spectrometer.
3. Electrosprayed ions are injected into the ion trap.
4. The precursors are mass-selected and stored in the trap.
5. Upon reaching a desired ion capacity, the beam shutter opens and the irradiation starts.
6. The shutter closes after the predefined irradiation time.
7. A tandem mass spectrum is generated by ejecting the produced ions.
8. The beamline is set to the next photon energy value and the whole procedure is repeated for a desired energy range in order to obtain relative ion yields as a function of energy.

The Thermo Scientific's Xcalibur™ software, used for controlling the experimental parameters, was also used for recording the results. The first step consists of identifying the dominant peaks in the recorded mass spectra and determining whether they correspond to precursor, SI or DI ions. It is important to carefully choose adequate ranges of m/z values around each peak according to its shape, which will be used for obtaining relative SI and DI ion yields as a function of the photon energy. The relative energy dependencies of SI and DI ion yields are extracted from the selected spectra as an area under the selected peaks, using a home-made script coded in Matlab®. All partial ion yields are normalized to both the total ion current (TIC) and the photon flux. The photon flux was measured under the same experimental conditions for this purpose. Graphical representations of results were generated with OriginLab® software.

3. Results and discussion

3.1. Action spectroscopy of protonated Substance P

3.2.1. C-edge

Mass spectra were recorded for three photon activation energy values: 283 eV, 288 eV and 293 eV. The resulting mass spectra are shown in figure 3.1. The DI intensity is much smaller than the SI intensity for all three energies. It is also evident that the ionization of the precursor for 283 eV is far lower than for 288 eV and 293 eV.

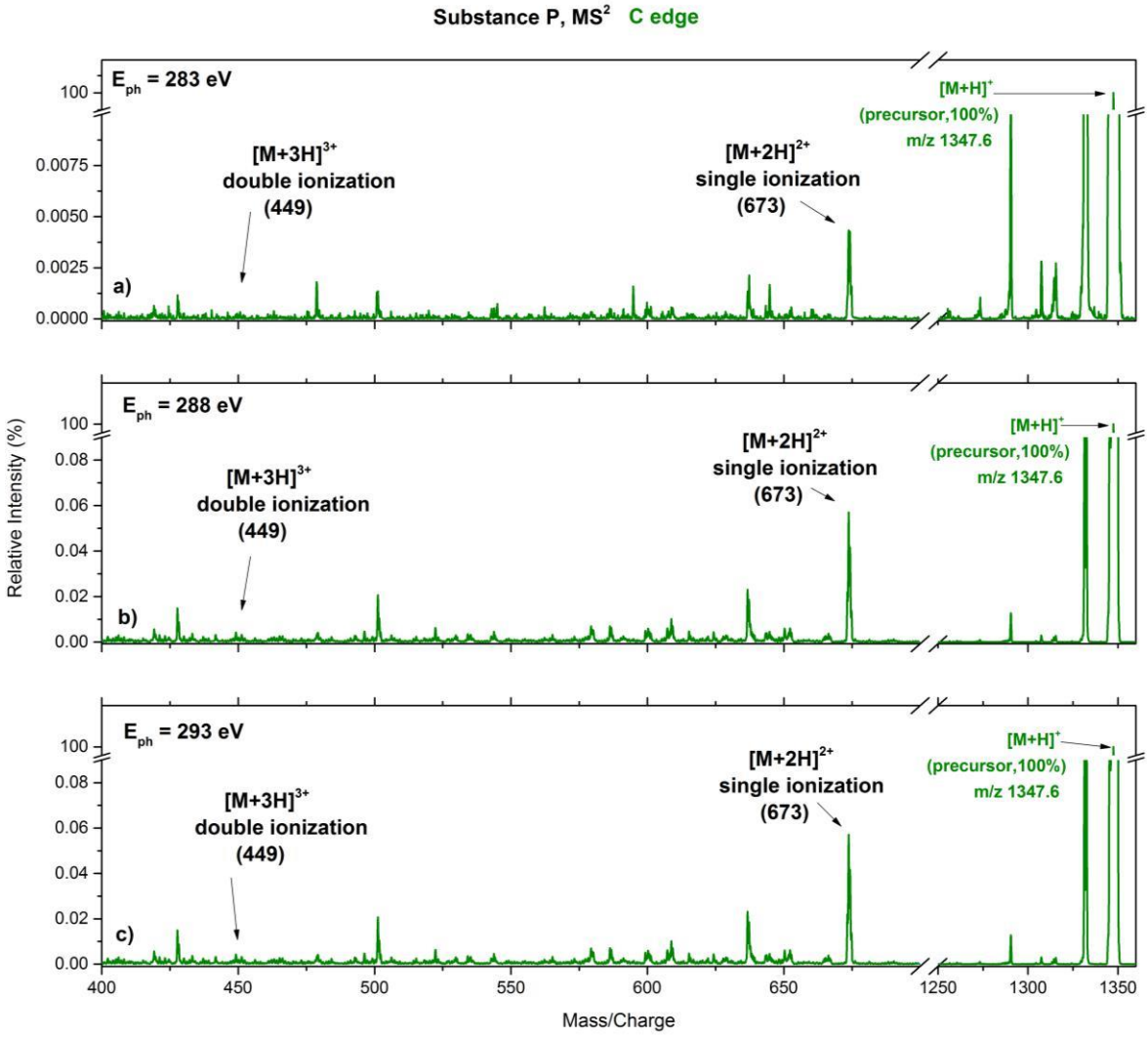

Figure 3.1.: C-edge mass spectra of protonated Substance P ([M+H]+, m/z 1347) for energy values: a) 283 eV, b) 288 eV and c) 293 eV.

3.2.2. N-edge

Mass spectra corresponding to the photon energies of 396 eV (below the 1s → π^*_{amide} resonance), 401 eV (at the 1s → π^*_{amide} resonance) and 409 eV (above the 1s → π^*_{amide} resonance) are shown in figure 3.5. Except distinguished peaks corresponding to SI and DI of the precursor, one can see a rich fragmentation pattern. However, a detailed discussion of the fragmentation pattern is out of scope of this work, which is focused on the action NEXAFS spectroscopy. Figure 3.2 clearly shows that intensity of the peaks is not the same for different energies, so the fragmentation pattern depends on the activation photon energy.

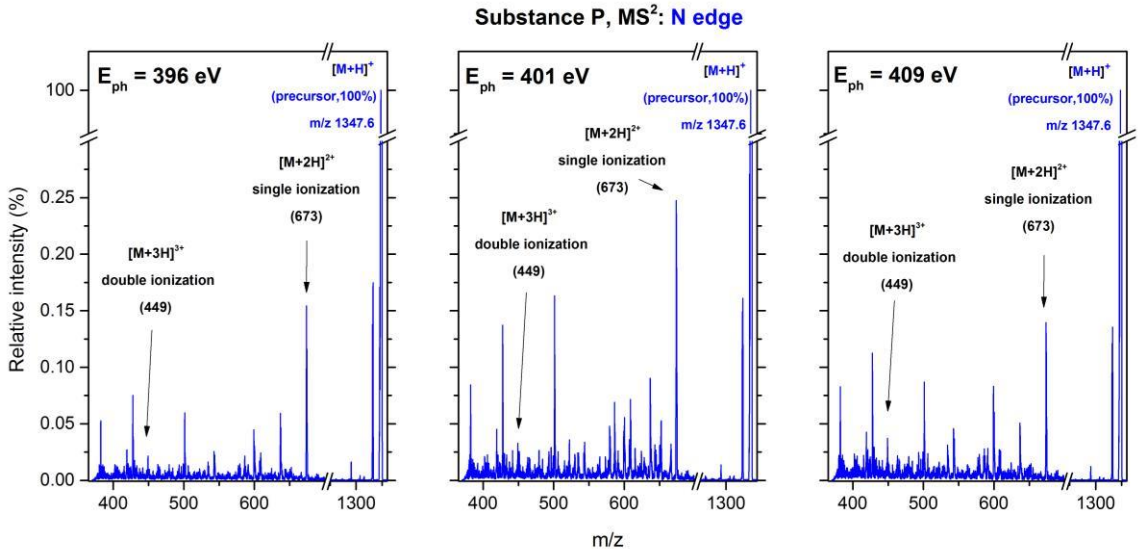

Figure 3.2: N-edge mass spectra of protonated Substance P ([M+H]+, m/z 1347) for energy values: 396 eV, 401eV and 409 eV.

The N-edge action spectrum was obtained by recording mass spectra while irradiating the protonated Substance P precursor with photons in the energy range 397 eV – 409 eV, with an energy step of 1eV. The partial ion yield spectra for SI and DI, extracted from the mass spectra, are shown in figure 3.3.

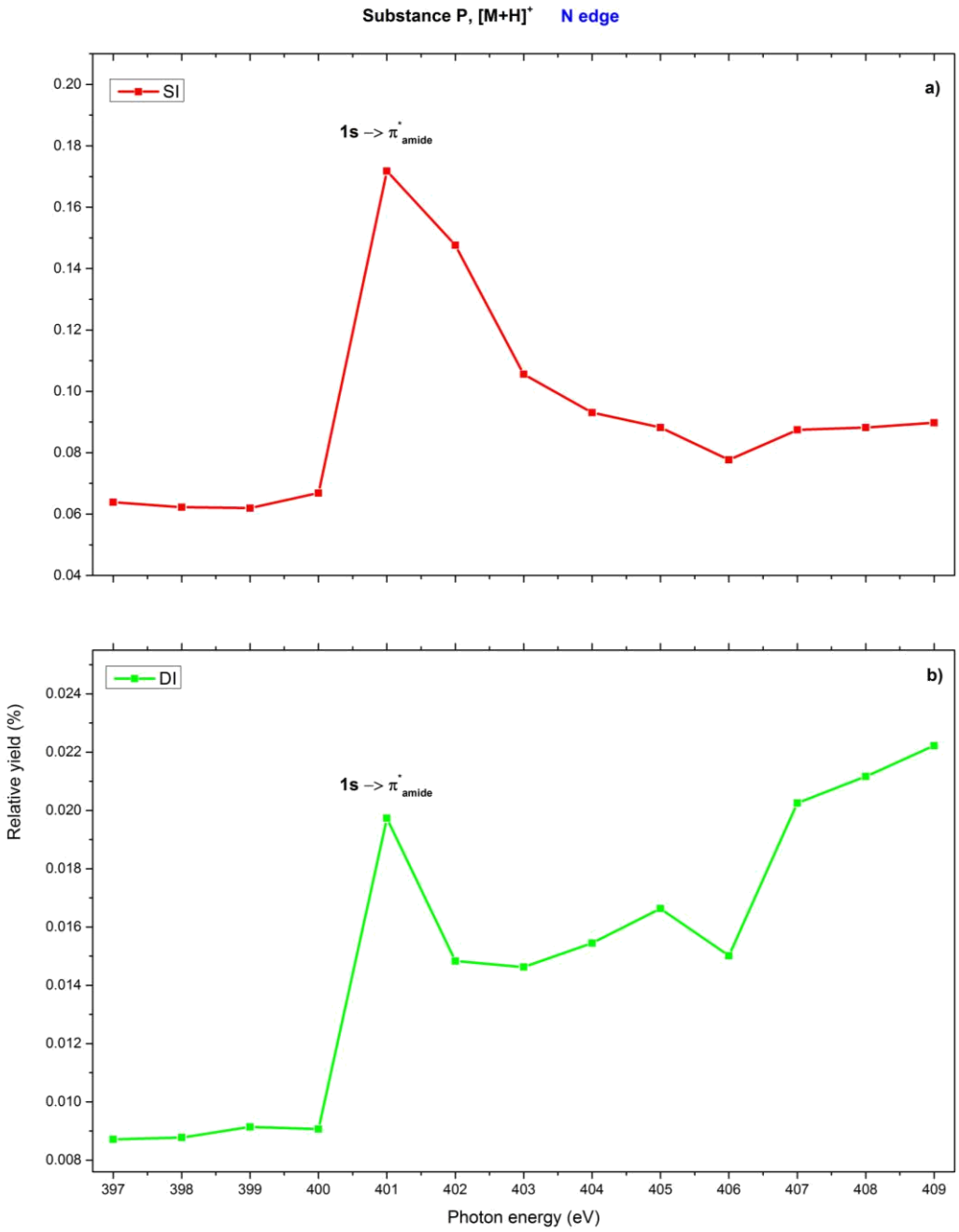

Figure 3.3: The N-edge action spectra of protonated Substance P: a) Partial ion yield for SI ($[M+2H]^{2+}$, m/z 673); b) Partial ion yield for DI ($[M+3H]^{3+}$, m/z 449).

The peak at about 401 eV, seen on both SI and DI ion yield spectra, corresponds to an electronic transition from an 1s N electron to the π^*_{amide} antibonding molecular orbital of the peptide bond C=O.[2] The DI (figure 3.3. b) increases with the increase of the photon energy above the resonance due to the opening a direct K-shell ionization channel.

3.2.3. O-edge

Mass spectra of protonated bare Substance P precursors were recorded for four photon activation energies: 526 eV, 531 eV, 539 eV and 544 eV (see figure 3.4). Evidently, the intensity of the peaks differs for different energy values, demonstrating that the fragmentation pattern is a function of the photon activation energy.

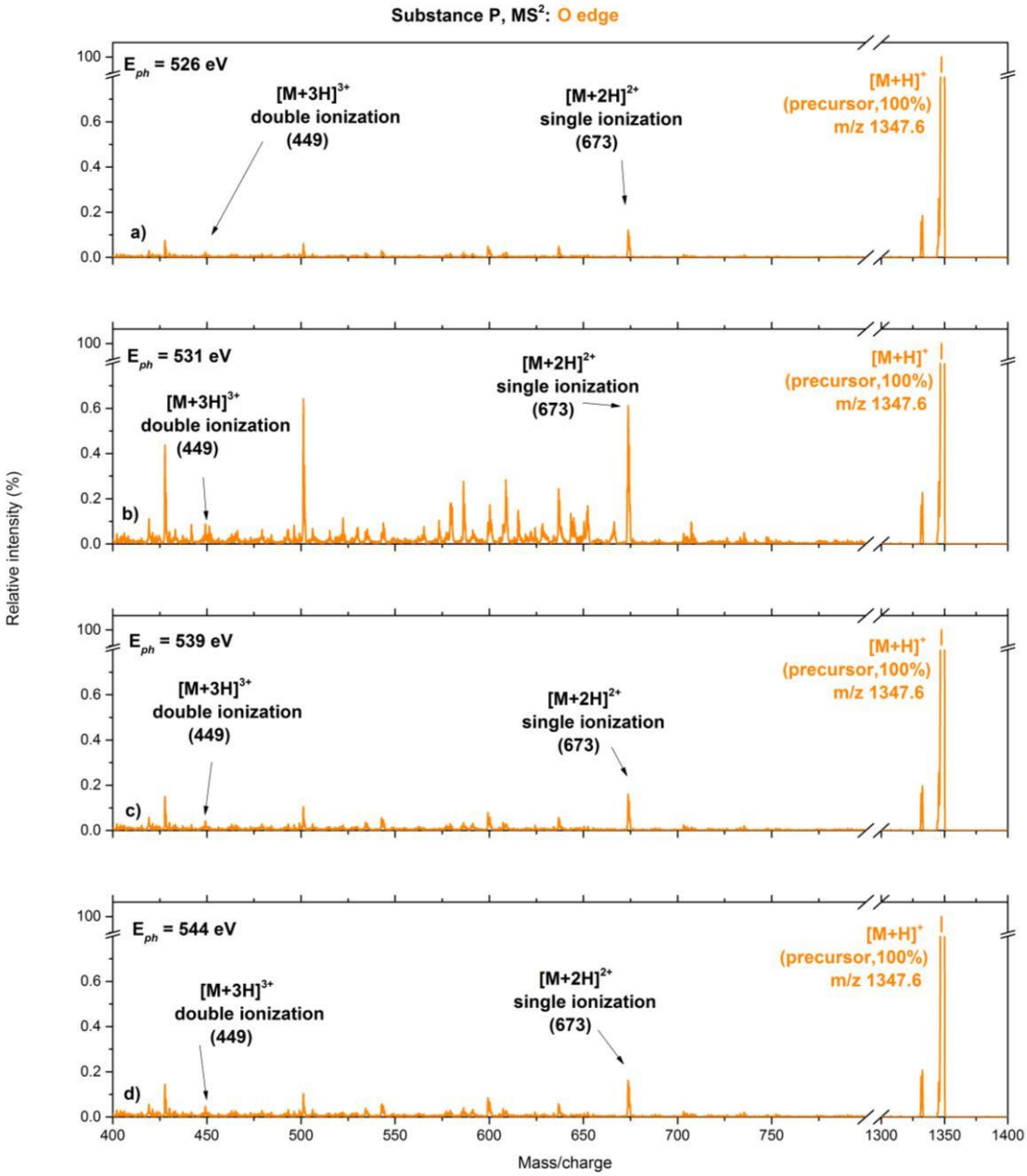

Figure 3.4: O-edge mass spectra of protonated Substance P ([M+H]+, m/z 1347) for energy values: a) 526 eV, b) 531eV, c) 539 eV and d) 544 eV.

3.2. Collision-induced dissociation of nanoslvated Substance P

Production and isolation of nanosolvated ionic species by use of a commercial ESI source is very challenging. It demands a particular combination of the solution and ESI parameters, such as the concentration of the solution, transfer tube temperature, voltages, sheath gas flow rate etc. Typically, target ions densities of nanosolvated precursors are orders of magnitude lower than of the bare precursor. Therefore, it is very important to insure negligible influence of background species.

In order to check for successful nanosolvation of protonated Substance P, we needed to demonstrate that the hydrated precursors $[M+kH_2O+nH]^{n+}$ go through collision--induced dissociation (CID) by losing water molecules. Therefore, we subjected several samples to CID and analyzed the resulting ions using several levels of tandem mass spectrometry. From a physical standpoint, the CID procedure involves inelastic collisions of precursor ions with neutral helium atoms for a predefined period of time. Upon collision, the He atoms transfer energy to molecular ions, which can lead to bond breakage. The first bonds that break are the weakest ones, which are, in our case, the bonds connecting the water molecules and Substance P. In tandem mass spectrometry, the process may be repeated a number of times. In our case, the CID mass spectra are expected to have peaks which correspond to precursor ions and the ions generated by water losses. Our results confirm this assumption. We performed CID for several precursors, hydrated with a different number of water molecules, as well as different collisional energy values. Peaks corresponding to water losses can be clearly identified in the CID mass spectra obtained in our measurements, confirming the presumption of nanosolvation.

Figure 3.5 shows the CID spectra for doubly hydrated, doubly protonated precursor ions $[M+2H_2O+2H]^{2+}$ (m/z 683), recorded under the following distinct experimental conditions:

- precursor ions are only preserved in the trap under normal conditions, recording time 600 ms, with the isolation width (iw) 1 (figure 3.5 a)
- increased collisional energy (CID conditions), recording time 600 ms, iw = 1 (figure 3.5 b)

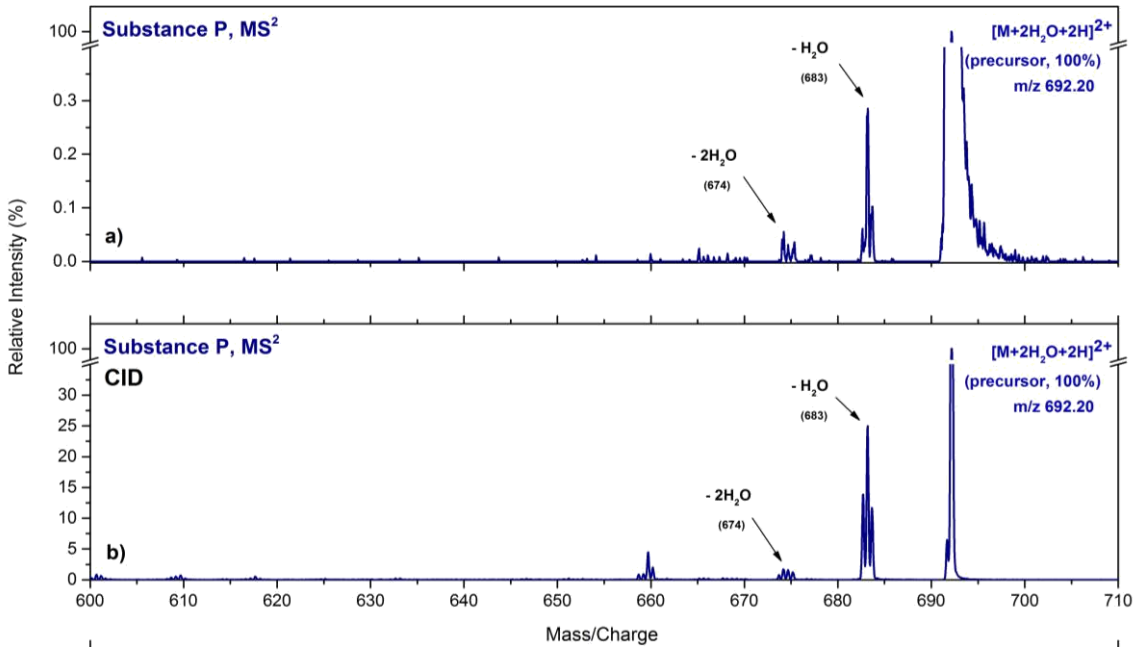

Figure 3.5: CID MS^2 spectra for doubly hydrated precursor ions $[M+2H_2O+2H]^{2+}$ (m/z 683).
(a) The spectrum was recorded for 600 ms with an isolation width 1, under normal trapping conditions.
(b) The spectrum was recorded for 600 ms with an isolation width 1, for increased collisional energy.

The results indicate that the precursor nanosolvated ions can lose water molecules even by just preserving them in the trap (tentatively, we can explain this by collision and (or) black body radiation-induced evaporation). However, the abundance of singly and doubly dehydrated ions significantly increased (by one order of magnitude) when the precursor was subjected to CID.

The CID MS^2 spectrum of a nine time hydrated doubly protonated precursor ion of Substance P $[M+9H_2O+2H]^{2+}$ (m/z 755) is shown in figure 3.6. The spectrum was recorded for 30 ms with an isolation width 2. Another CID spectrum worth mentioning is the spectrum obtained by recording precursor ions with 30 solvent molecules $[M+30H_2O+2H]^{2+}$ (m/z 944) for 30 ms with an isolation width 2, is displayed in figure 3.7. These results also clearly indicate that CID fragmentation predominantly occurs by losing water.

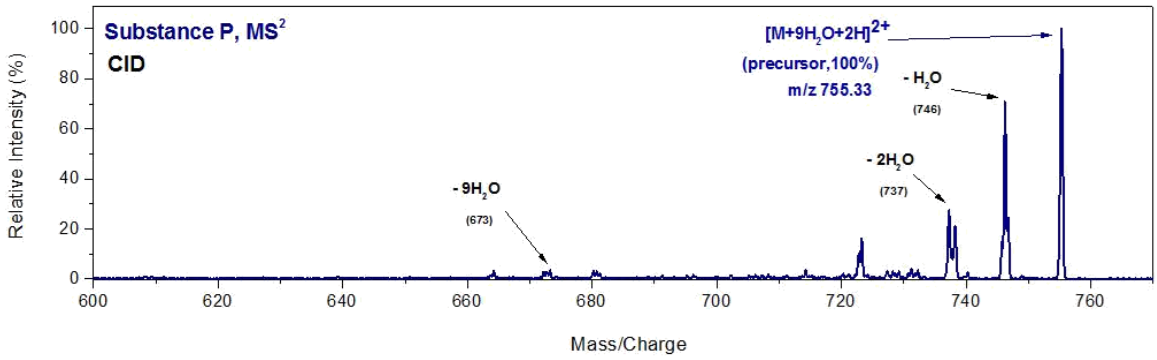

Figure 3.6: The CID spectrum for nine times hydrated $[M+9H_2O+2H]^{2+}$ precursor ions (m/z 755). The spectrum was recorded for 30 ms with an isolation width 2.

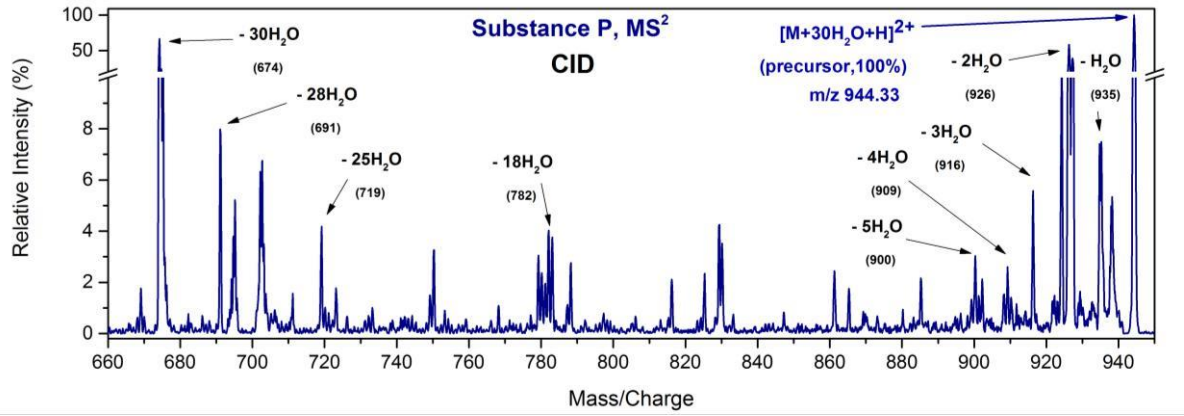

Figure 3.7: The CID spectrum for thirty times hydrated $[M+30H_2O+2H]^{2+}$ precursor ions (m/z 755). The spectrum was recorded for 30 ms with an isolation width 1.5.

In conclusion, the CID tests confirm that we can produce nanosolvated protonated Substance P precursors and isolate them in the ion trap in order to perform action NEXAFS spectroscopy.

3.3. Action spectroscopy of nanosolvated protonated Substance P around O K-edge

To gain insight into the effects of nanosolvation on the fragmentation of protonated Substance P, we recorded tandem mass spectra at different photon energies around the O K-edge for Substance P precursor nanosolvated with 11 water molecules. It should be noted, however, that due to very low target density and low cross sections (due to relatively small number of oxygen atoms in the molecule) signal to noise ratio is very small, forcing us to reduce the number of points and the photon energy resolution. Still, according to our knowledge, such experimental investigation has never been performed previously, therefore, the results could be very important to stimulate further research that could lead to better understanding of the charactersitics of nanosolvated peptides. For example, one of the first questions arises whether we can detect separate spectroscopic signatures from the peptide itself and the water cluster. If, at all, attached water molecules forms a cluster. With this in mind, action NEXAFS spectroscopy around O K-edge might be very powerful since the excited 1s electron can belong either to peptide bond oxygen atom or a water oxygen atom.

In any case, the excitation and subsequent ionization of the nanosolvated molecule will lead to water loss. Therefore, recording the total ion yield for an m/z range, chosen to encompass all losses of water molecules initially attached to the precursor, we can measure total water losses as a function of the photon energy. We expect that increased water loss appears upon excitation of the O K-shell.

Figure 3.8. presents a total water loss of a doubly protonated Substance P ion solvated with eleven water molecules $[M+2H+11H_2O]^{2+}$ (m/z 773.5), covering the m/z range 674-766. According to previous action NEXAFS of peptides and proteins[1], the 531 eV peak corresponds to the excitation of an oxygen core electron into the antibonding C=O

π^* molecular orbital corresponding to the peptide bond. On the other hand, the 535 eV peak should correspond to the energy at which water clusters resonantly absorb photons[44], due to the excitations into water molecular orbitals. Therefore, in the first case the photons are absorbed by the peptide, while they are absorbed by water molecules in the latter case.

.

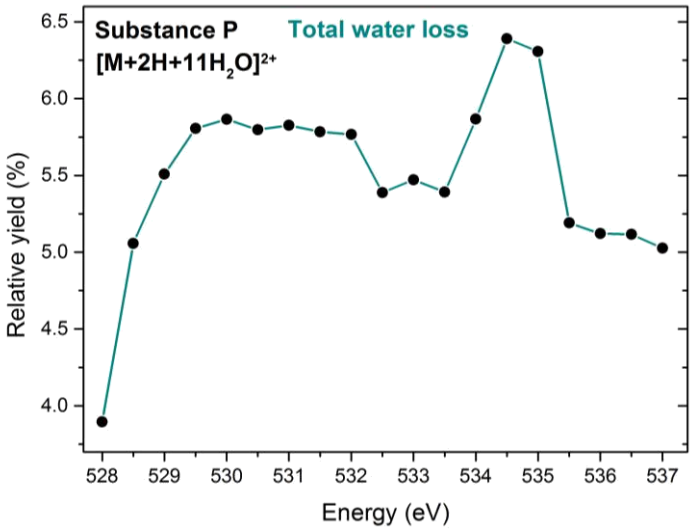

Figure 3.8: The total water loss from a doubly protonated nanosolvated substance P precursor $[M+2H+11H_2O]^{2+}$ (m/z 773).

Relaxation may occur by releasing water molecules, as can be seen in the mass spectra (see figure 3.9). Also, it is worth noting that compared to doubly protonated bare precursors, hydrated precursors have more intense water losses (see figure 3.10 whichshows total water losses of the doubly ionized precursor $[M+2H]^{2+}$ for comparison).

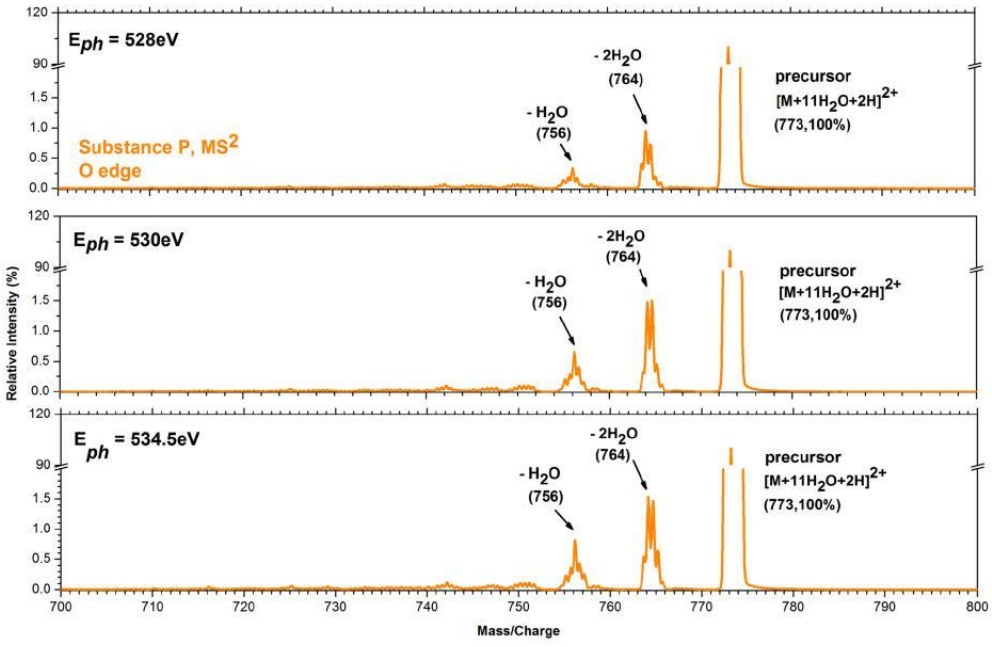

Figure 3.9: Water losses from the doubly protonated nanosolvated Substance P precursor ($[M+2H+11H_2O]^{2+}$, m/z 773) at 528 eV, 530 eV and 534.5 eV.

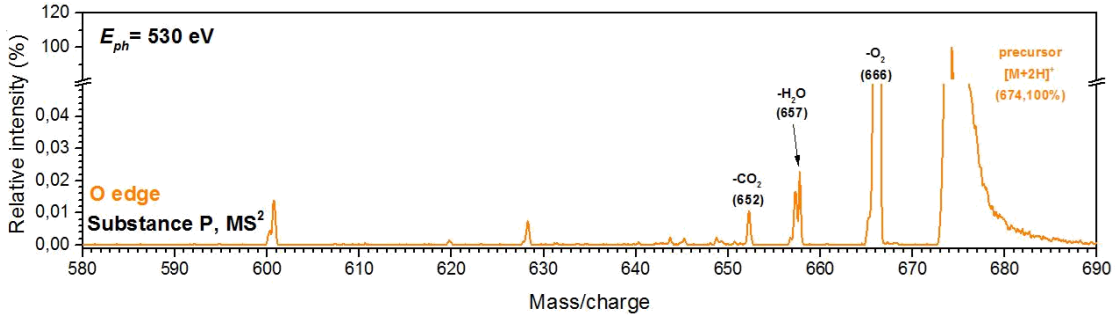

Figure 3.10: Water losses from the doubly protonated non-solvated Substance P precursor ($[M+2H]^{2+}$, m/z 674) at 530 eV.

We will also present mass spectra for the precursor $[M+2H+30H_2O]^{2+}$ at the energies 529 eV and 534 eV (figure 3.11). In this case, the precursor also relaxes by releasing molecules of water, characterized by two distinct peaks, which can be identified. It is interesting to note that water loss is much more efficient at 534 eV (figure 3.11 b), which is close to the enegy at which 1s oxygen electrons are resonantly captured by molecular orbitals of water, than at 529 eV, which is below both resonant energies.

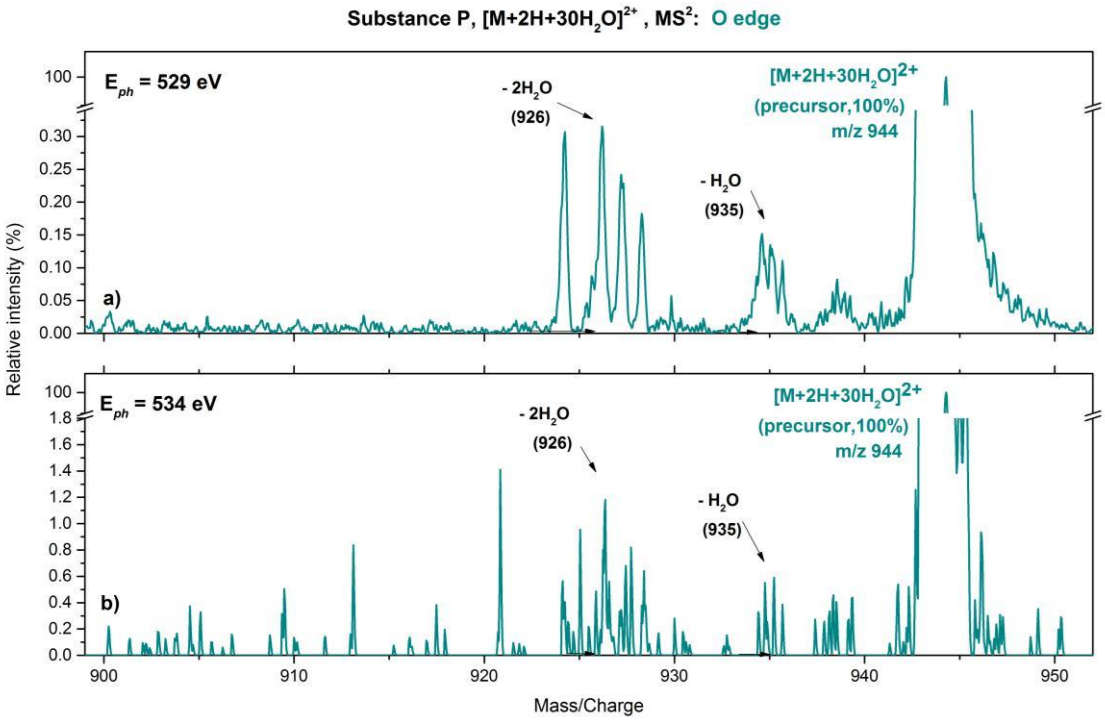

Figure 3.11: Water losses from the doubly protonated nanosolvated Substance P precursor ($[M+2H+30H_2O]^{2+}$, m/z 944) at a) 529 eV and b) 534 eV.

4. Conclusion

Mass spectra for energies below, above and at the resonance for C, N and O K edges of protonated Substance P precursors indicate that the intensity of the peaks in the spectra is a function of the activation photon energy. The intensities depend on both which K edge is probed and whether the activation energy is below, at or above the resonance excitation energies.

The NEXAFS action spectra for the N-edge of Substance P confirms a possibility to record resonant transition of the 1s N electron to the peptide bond amide molecular orbital at about 401 eV. The contribution from direct K-shell ionization can be clearly seen in the DI action spectrum, but more detailed measurements are needed to evaluate the ionization threshold.

The performed CID tests for precursors hydrated with a controlled number of water molecules have shown that we have successfully produced and preserved in the ion trap nanosolvated protonated Substance P precursors.

Despite reduced signal to noise ratio due to low target density, tandem mass spectra around the O K-edge of a doubly protonated Substance P ion nanosolvated with 11 molecules of water reveal that it is possible to detect two distinct resonances in the ion yield spectra corresponding to total water loss. The first resonant energy (531 eV) corresponds to the resonant transition of a 1s O electron into the antibonding amide orbital of the peptide bond. The second resonant energy (535 eV) corresponds to the transition of a 1s O electron into a molecular orbital of a water cluster. Future work in this aspect should be focused on improving signal to noise ratio, allowing to improve the photon energy resolution and perform more detailed research.

5. References

1. Milosavljević AR, Canon F, Nicolas C, Miron C, Nahon L, Giuliani A. Gas-phase protein inner-shell spectroscopy by coupling an ion trap with a soft X-ray beamline. *J Phys Chem Lett*. 2012;3:1191-1196. doi:10.1021/jz300324z.
2. Milosavljević AR, Nicolas C, Ranković ML, Canon F, Miron C, Giuliani A. K-Shell Excitation and Ionization of a Gas-Phase Protein: Interplay between Electronic Structure and Protein Folding. *J Phys Chem Lett*. 2015;6(16):3132-3138. doi:10.1021/acs.jpclett.5b01288.
3. Milosavljević AR, Cerovski VZ, Canon F, Nahon L, Giuliani A. Nanosolvation-Induced Stabilization of a Protonated Peptide Dimer Isolated in the Gas Phase. *Angew Chemie Int Ed*. 2013;52(28):7286-7290. doi:10.1002/anie.201301667.
4. Hähner G. Near edge X-ray absorption fine structure spectroscopy as a tool to probe electronic and structural properties of thin organic films and liquids. *Chem Soc Rev*. 2006;35(12):1244. doi:10.1039/b509853j.
5. Gas-Phase Near-Edge X-ray Absorption Fine Structure (NEXAFS) Spectroscopy of Nanoparticles, Biopolymers and Ionic Species, Aleksandar R. Milosavljević, Alexandre Giuliani & Christophe Nicolas, in *Nanoscience and Nanotechnology*, Vol. **5**: X-ray and Neutron Techniques for Nanomaterials Characterization, edited by Prof. Dr. Challa S.S.R. Kumar, Springer-Verlag Berlin Heidelberg (2015, in press)
6. Milosavljević AR, Cerovski VZ, Canon F, et al. Energy-Dependent UV Photodissociation of Gas-Phase Adenosine Monophosphate Nucleotide Ions: The Role of a Single Solvent Molecule. *J Phys Chem Lett*. 2014;5(Figure 1):1994-1999. doi:10.1021/jz500696b.
7. Otto R, Brox J, Trippel S, Stei M, Best T, Wester R. Single solvent molecules can affect the dynamics of substitution reactions. *Nat Chem*. 2012;4(7):534-538. doi:10.1038/nchem.1362.
8. Doi K, Togano E, Xantheas SS, et al. Microhydration effects on the intermediates of the SN2 reaction of iodide anion with methyl iodide. *Angew Chemie - Int Ed*. 2013;52:4380-4383. doi:10.1002/anie.201207697.

9. Nagornova NS, Rizzo TR, Boyarkin O V. Interplay of intra- and intermolecular H-bonding in a progressively solvated macrocyclic peptide. *Science*. 2012;336(6079):320-323. doi:10.1126/science.1218709.

10. XANES: Theory - Chemwiki. http://chemwiki.ucdavis.edu/Physical_Chemistry/Spectroscopy/X-ray_Spectroscopy/XANES%3A_Theory. Accessed October 14, 2015.

11. NEXAFS Spectroscopy (stanford.edu). https://www-ssrl.slac.stanford.edu/stohr/nexafs.htm. Accessed October 14, 2015.

12. Kebarle P, Verkerk U. ELECTROSPRAY: FROM IONS IN SOLUTION TO IONS IN THE GAS PHASE, WHAT WE KNOW NOW. *Mass Spectrom Rev*. 2009;(28):898-917. doi:10.1002/mas.20247.

13. The Nobel Prize in Chemistry 2002. http://www.nobelprize.org/nobel_prizes/chemistry/laureates/2002/. Accessed October 14, 2015.

14. Protein Structure: Introduction. http://lectures.molgen.mpg.de/ProteinStructure/Intro/. Accessed October 18, 2015.

15. Gold V. *IUPAC Compendium of Chemical Terminology*. 2nd ed. (McNaught AD, Wilkinson A, eds.). Oxford: Blackwell Scientific Publications; 1997. doi:10.1351/goldbook.

16. Moss GP, Smith P a S, Tavernier D. Glossary of Class Names of Organic Compounds and Reactive Intermediates Based on Structure. *Pure Appl Chem*. 1995;67:1307-1375. doi:10.1351/pac199567081307.

17. Peptide Guide: The Peptide Bond. http://www.peptideguide.com/peptide-bond.html. Accessed October 18, 2015.

18. Kim K, Seong BL. Peptide Amidation: Production of Peptide Hormones in vivo and in vitro. *Biotechnol Bioprocess Eng*. 2001;6(4):244-251. doi:10.1007/BF02931985.

19. Datar P, Srivastava S, Coutinho E, Govil G. Substance P: structure, function, and therapeutics. *Curr Top Med Chem*. 2004;4(1):75-103. doi:10.2174/1568026043451636.

20. ChemSpider: Substance P. http://www.chemspider.com/Chemical-Structure.33558.html. Accessed October 18, 2015.

21. Harrison S, Geppetti P. Substance p. *Int J Biochem Cell Biol*. 2001;33(6):555-576. doi:10.1016/S1357-2725(01)00031-0.

22. De Felipe C, Herrero JF, O'Brien JA, et al. Altered nociception, analgesia and aggression in mice lacking the receptor for substance P. *Nature*. 1998;392(6674):394-397. doi:10.1038/32904.

23. O'Connor TM, O'Connell J, O'Brien DI, Goode T, Bredin CP, Shanahan F. The role of substance P in inflammatory disease. *J Cell Physiol*. 2004;201(2):167-180. doi:10.1002/jcp.20061.

24. Abbadie C, Brown JL, Mantyh PW, Basbaum a I. Spinal cord substance P receptor immunoreactivity increases in both inflammatory and nerve injury models of persistent pain. *Neuroscience*. 1996;70(1):201-209. doi:10.1016/0306-4522(95)00343-H.

25. Ebner K, Singewald N. The role of substance P in stress and anxiety responses. *Amino Acids*. 2006;31(3):251-272. doi:10.1007/s00726-006-0335-9.

26. Geracioti TD, Carpenter LL, Owens MJ, et al. Elevated Cerebrospinal Fluid Substance P Concentrations in Posttraumatic Stress Disorder and Major Depression. *Am J Psychiatry*. 2006;163(4):637-643. doi:10.1176/appi.ajp.163.4.637.

27. Kramer MS, Winokur A, Kelsey J, et al. Demonstration of the Efficacy and Safety of a Novel Substance P (NK1) Receptor Antagonist in Major Depression. *Neuropsychopharmacology*. 2004;29(2):385-392. doi:10.1038/sj.npp.1300260.

28. Canon F, Milosavljević AR, Nahon L, Giuliani A. Action spectroscopy of a protonated peptide in the ultraviolet range. *Phys Chem Chem Phys*. 2015;17(39):25725-25733. doi:10.1039/C4CP04762A.

29. Demartini DR. A Short Overview of the Components in Mass Spectrometry Instrumentation for Proteomics Analyses. *Tandem Mass Spectrom - Mol Charact*. 2013;1. doi:10.5772/54484.

30. Kuhlicke A, Partner H. Nano-probes and Nano-particles. https://www.physik.hu-berlin.de/de/nano/research/nanoprobesparticles/nanoprobesparticles. Accessed October 7, 2015.

31. Dawson PH, York A. *Quadrupole Mass Spectrometry and Its Applications*. Amsterdam: Elsevier Scientific Publishing Company; 1976.

32. Thermo Scientific. http://www.thermoscientific.com/en/home.html. Accessed October 14, 2015.

33. Mass Spectrometry Tutorial | Chemical Instrumentation Facility. http://www.cif.iastate.edu/mass-spec/ms-tutorial. Accessed October 7, 2015.

34. Dass C. *Fundamentals of Mass Spectrometry*. Hoboken, New Jersey: John Wiley & Sons, Inc; 2007

35. Finnigan^{TM} LTQ^{TM} Hardware Manual. 2003.

36. SOLEIL in 3 questions. http://www.synchrotron-soleil.fr/portal/page/portal/RessourcesPedagogiques/Soleil3Questions. Accessed October 2, 2015.

37. Synchrotron Soleil, Wikimedia Commons. https://commons.wikimedia.org/wiki/Synchrotron_Soleil#/media/File:Sch%C3%A9ma_de_principe_du_synchrotron.jpg. Accessed October 1, 2015.

38. About SOLEIL. http://www.synchrotron-soleil.fr/images/File/recherche/Bibliotheque/DocumentationEnLigne/about-soleil.pdf. Accessed October 1, 2015.

39. Exploring Matter by the Light of SOLEIL. http://www.synchrotron-soleil.fr/images/File/recherche/Bibliotheque/DocumentationEnLigne/PosterLumiere - A.pdf. Accessed October 2, 2015.

40. PLÉIADES beamline. http://www.synchrotron-soleil.fr/Recherche/LignesLumiere/PLEIADES. Accessed October 1, 2015.

41. PLEIADES beamline description. http://www.synchrotron-soleil.fr/images/File/recherche/ligneslumiere/pleiades/Beamlines-description-Pleiades.pdf. Accessed October 1, 2015.

42. Milosavljević AR, Nicolas C, Lemaire J, et al. Photoionization of a protein isolated in vacuo. *Phys Chem Chem Phys*. 2011;13(34):15432. doi:10.1039/c1cp21211g.

43. Milosavljević AR, Nicolas C, Gil J-F, et al. VUV synchrotron radiation: a new activation technique for tandem mass spectrometry. *J Synchrotron Radiat*. 2012;19(2):174-178. doi:10.1107/S0909049512001057.

44. Wernet P, Nordlund D, Bergmann U, et al. The structure of the first coordination shell in liquid water. *Science*. 2004;304(5673):995-999. doi:10.1126/science.1096205.